FEATURE ARTICLE

Broadening and Shifts of Vibrational Bands Due to the Effect of Thermal Chemical Reactions

Kurt A. Wood† and Herbert L. Strauss*

Department of Chemistry, University of California, Berkeley, California 94720 *(Received: February 2, 1990)*

The effect of thermal chemical reactions on vibrational spectra is discussed qualitatively by contrasting vibrational spectra with magnetic resonance spectra. The difference in time scale characteristic of each type of spectra leads to very different effects of reaction. Ordinary thermal reactions do not have a fast enough "transit time"—time spent in the transition state—to lead to a simple effect on vibrational spectra. As a consequence, obtaining reaction rates from the broadening or shift of vibrational bands requires detailed knowledge of the other broadening/shift mechanisms involved, and this makes the analysis difficult. The qualitative effect of fast reactions is illustrated by means of "Kubo diagrams" in which the band behavior is plotted as a function of the Kubo parameters. It is pointed out that one important case of vibrational spectra for which exchange coupling does lead to the magnetic resonance/Bloch equation result occurs at very low temperatures where only four energy levels are involved. Here the exchange involved is *not* due to a chemical reaction. The process of pseudocollapse is identified as the progressive broadening of bands arising from an anharmonic potential, which leads to shifts having no direct relation to reaction rates. References are provided to correct treatments of the effects of reaction rates.

I. Introduction

Vibrational spectra are often observed arising from molecules that undergo rapid reactions. Sometimes, as conditions change to make reactions faster, these bands broaden. More intriguing are situations in which there are multiple bands that merge as the reactions become faster. In these circumstances, it is natural to attribute the broadening to the reaction-limited lifetime of the reacting species and to interpret merging of the bands in the manner much used for analyzing magnetic resonance spectra. The rate of reaction can then be determined by applying standard (although not necessarily simple) methods of spectral analysis. However, such an analysis assumes that the time during which the molecule is between the starting site (reactant) and the ending site (product) is very short compared to the reciprocal of the frequencies characteristic of the spectra. This assumption is usually excellent in magnetic resonance. For reactions whose rate is determined by thermal nuclear motion on a ground-state electronic potential, it is quite incorrect in vibrational spectroscopy. Reactions that occur thermally on ground-state electronic surfaces have often been investigated by vibrational spectroscopy. Examples are reactions that involve (1) rotation of a given group such as OH in ethanol, SO_4^{2-} in potassium alum $[KAl(SO_4)_2 \cdot 2H_2O]$, or methyl groups in chain molecules and (2) transfer of atoms or molecules such as occur with the ionization of an acid or the dissociation of a charge-transfer complex. All of these reactions are characterized by a transit time τ_t, which is fast on a magnetic resonance time scale but slow on a vibrational time scale. (For reactions for which transition-state theory holds, τ_t is approximately the time spent in the transition state.)

The goal of a magnetic resonance like analysis is often to determine the reaction rate. However, the difference between the time scales of the two spectroscopies means that the mechanisms that lead to the shift and broadening of vibrational bands are quite different than those that lead to changes in magnetic resonance bands. As a consequence, it turns out that the rate of reaction *cannot* be estimated in a straightforward manner from the spectra.

There is a related phenomenon that often results in the broadening or shift of spectral lines—the exchange of the system between two spectral transitions. Each transition is between distinct energy levels and is represented by an off-diagonal element of the density matrix. Since we are here talking about exchange between distinct levels, this process is not a chemical reaction and no intermediate state "between" the levels is involved. For these situations, the magnetic resonance formalisms apply, for example, in the form of the Bloch equations. In certain limits, a reacting system can be modeled as an exchange between levels and, under these very limited circumstances, "exchange theory" will in fact apply. As we shall discuss, those limits for vibrational transitions usually involve very low temperatures and not the ordinary chemical situation.

The theme of this article is that very stringent conditions must be met in order to use simple theories to interpret the vibrational spectra of reacting systems. Since these conditions are rarely met in practice, more complex theories are necessary. To obtain chemical reaction rates from the application of these more complex theories to experimental spectra requires a detailed understanding of the other relaxation mechanisms that affect the spectra. Obtaining this ancillary information is a challenge.

We first provide an elementary discussion of the general features of line shapes, a discussion that will be a review for many readers. We continue with an outline of the standard treatment of chemical reaction systems as studied by magnetic resonance. Having prepared the background, we then discuss vibrational spectra, first those with relaxation in one potential well and then those with multiple wells. We summarize the results of these considerations with diagrams that list the spectral effects as functions of the relaxation rates of the system. One particularly important and often observed phenomenon, "pseudocollapse", is then discussed. Finally, we present our conclusions.

II. General Features of Line Shapes

The correlation function formulation of spectral phenomena shows most explicitly the relationships among the different types of rate processes, and so this is the formulation we will use. The intensity of a transition is equal to

$$I(\omega) = A\int_{-\infty}^{\infty} dt\, e^{-i\omega t}\langle[\mathbf{E}_0\cdot\mu(t)][\mathbf{E}_0\cdot\mu(0)]\rangle$$

Here the dipole moment, μ, interacts with the radiation represented by the amplitude of the field, $\mathbf{E}_0$. In many cases, the molecule

† Present address: Rohm and Haas, 727 Norristown Rd., Springhouse, PA 19477.

* To whom correspondence should be addressed.

0022-3654/90/2094-5677$02.50/0

changes orientation in the course of a reaction and so the angular part of eq 1 needs to be treated with care. For an isotropic sample, eq 1 reduces to the more familiar form[1]

$$I(\omega) = \frac{A|E_0|^2}{3}\int_{-\infty}^{\infty} dt\, e^{-i\omega t}\langle \mu(t)\cdot\mu(0)\rangle \qquad (1)$$

In words, the intensity is proportional to the Fourier transform of the correlation function of the dipole moment. The angular brackets imply an ensemble average, and quantum mechanical expectation values are understood. The frequency, ω, is in rad/s. The proportionality constant A contains the population of the various states and thus depends on temperature as well as frequency.

For other types of transitions, the dipole moment correlation function must be replaced with the appropriate transition moment correlation function. For example, for Raman spectroscopy, the possibilities are the isotropic or anisotropic parts of the polarizability.[2] We consider only systems that are spatially isotropic. In general, the appropriate correlation function is for one of the irreducible tensor components of the transition operator.

The moment associated with a dipole-allowed vibrational transition can usually be written as

$$\mu(t) = \mu_0 + \sum_j (\partial\mu/\partial q_j)_{q=0}\, q_j(t) \qquad (2)$$

which is summed over all the normal modes, q_j, and gives

$$I_j(\omega) \propto \int dt\, e^{-i\omega t}\langle q_j(t)\, q_j^*(0)\rangle \qquad (3)$$

for the jth band.

We can define the vibrational frequency $\omega(t)$ by

$$\dot{q}(t) = dq(t)/dt = i\omega(t)\, q(t) \qquad (4)$$

and then eq 1 may be expressed as

$$I(\omega) \propto \int dt\, e^{-i\omega t}\left\langle \exp\left(i\int_0^t \omega(t')\, dt'\right)\right\rangle \qquad (5)$$

where the subscripts j corresponding to a given band are understood. We note that $\omega(t) = \omega_0 =$ constant produces a delta function line shape at ω_0. If the ensemble average envelope decays with time constant Γ, characteristic of the energy relaxation or T_1 process of a damped harmonic oscillator, then

$$\left\langle \exp\left(i\int_0^t \omega(t')\, dt'\right)\right\rangle = e^{i\omega_0 t}e^{-\Gamma|t|} \qquad (6)$$

and the line shape is Lorentzian:

$$I(\omega) = \frac{1}{\pi}\,\mathrm{Re}\left\{\frac{1}{i(\omega-\omega_0)+\Gamma}\right\} = \frac{1}{\pi}\,\frac{\Gamma}{(\omega-\omega_0)^2+\Gamma^2} \qquad (7)$$

We note that exponential decay of the correlation function occurs in many systems, even when there is no energy relaxation; we will see several examples below.

It is also possible to define general parameters that describe the phase or T_2 relaxation of any system. Following Kubo,[3] we divide $\omega(t)$ into a static and a fluctuating part

$$\omega(t) = \omega_0 + \delta\omega(t) \qquad (8)$$

where ω_0 is chosen such that $\langle\delta\omega(t)\rangle = 0$. Then the "modulation amplitude" Δ, the root mean square of the frequency fluctuation, is defined by

$$\Delta^2 = \langle[\delta\omega(t)]^2\rangle \qquad (9)$$

and the "modulation time" τ_c, the characteristic time that frequency fluctuations persist, is given by

$$\tau_c = (1/\Delta^2)\int_0^\infty dt\, \langle\delta\omega(t)\,\delta\omega(0)\rangle \qquad (10)$$

(1) Flygare, W. H. *Molecular Structure and Dynamics*; Prentice-Hall: Englewood Cliffs, NJ, 1978.
(2) MacPhail, R. A.; Strauss, H. L. *J. Chem. Phys.* **1985**, *82*, 1156.
(3) Kubo, R. In *Fluctuations, Relaxation and Resonance in Magnetic Systems*; Ter Haar, D., Ed.; Plenum: New York, 1962; p 23.

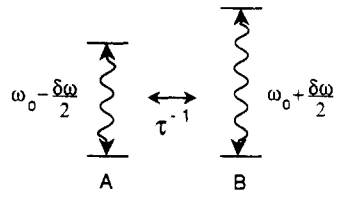

Figure 1. "Exchange" between a pair of two-level systems. This mechanism describes the effect of chemical reactions in nuclear magnetic resonance, for which A and B are two chemically distinct sites. The diagram is also applicable for the interaction between a vibrational fundamental A and its first hot band B. The restriction to the first hot band makes this diagram applicable only in the low-temperature limit. The wavy lines represent a radiation-induced transition, or coherent superposition, which is transferred from the A to the B set of states, or vice versa, by the "exchange" process denoted by the solid arrow. The frequencies of the transitions in the B and A sites are $\omega_0 \pm \delta\omega/2$, and the exchange rate is τ^{-1}. The transit time, τ_t, the time the system spends between A and B, is assumed to be much faster than any other times, that is, $\tau_t \ll \tau$, $\tau_t \ll 1/\delta\omega$.

The dimensionless "Kubo parameter" $\kappa \equiv \Delta\tau_c$ measures the relative rate of change of the oscillator frequency. For *slow modulation*, $\kappa \gg 1$, each individual oscillator has a constant frequency during the characteristic time of the experiment, and the band intensity profile simply reflects the static distribution of frequencies, $\omega_0 + \delta\omega$. For this situation, the half-width at half-height, $\Delta\omega_{1/2}$, is on the order of Δ.

On the other hand, for *fast modulation*, $\kappa \ll 1$, each individual oscillator samples the whole distribution of frequencies during the time scale of the experiment and oscillates at roughly the average frequency ω_0. The band profile is narrowed considerably (motional narrowing) and approaches a Lorentzian form, with $\Delta\omega_{1/2} = \Delta^2\tau_c = \Delta\kappa$. This is considerably less than the width in the slow modulation case, since $\Delta\kappa \ll \Delta$.

III. Chemical Exchange in Magnetic Resonance

The case of chemical exchange in NMR provides a good illustration of the use of the Kubo parameter to characterize a system. In the simplest case, that of a spin $^1/_2$ nucleus exchanging between two chemically distinct sites (which we will call "A" and "B"), the spin system is described by a pair of interacting "two-level systems", as shown in Figure 1. The two states in each two-level system correspond to the spin being up or down. The NMR radiation creates a phase coherence between the two levels, and this phase coherence is transferred between sites by the exchange process. A classic example is that of the methyl protons in *N*,*N*-dimethylformamide $[(CH_3)_2NCHO]$.[4] The methyl groups occupy two distinct sites, one cis and the other trans with respect to the aldehyde proton. In this case the chemical exchange process is the slow internal rotation about the N–C (aldehyde) bond. Calculated spectra as a function of reaction rate are shown in Figure 2.

If the frequencies of the NMR transitions in the B and A sites are $\omega_0 \pm \delta\omega/2$, respectively, and the exchange rate between the A and B sites is τ^{-1}, then the modulation parameters are

$$\Delta = |\delta\omega|/2 \quad \text{and} \quad \tau_c = \tau/2 \qquad (11)$$

When the chemical exchange is slow, i.e., $\tau^{-1} \ll \Delta$ or $\kappa \gg 1$, the NMR spectrum consists of two narrow lines at $\omega_0 \pm \delta\omega/2$. As the exchange rate increases, i.e., as κ becomes smaller, the lines broaden and shift toward one another until they merge into a single broad line when κ is on the order of one. For an increasingly faster exchange rate, i.e., for a further reduction of κ, the single line narrows more and more, eventually giving a Lorentzian band at ω_0, of width $\Delta\kappa = \Delta^2\tau_c$ for $\kappa \ll 1$ (Figure 2). Thus, for $\kappa \gg 1$,

(4) Kaplan, J. F.; Fraenkel, G. *NMR of Chemically Exchanging Systems*; Academic: New York, 1980. Slichter, C. P. *Principles of Magnetic Resonance*, 2nd ed.; Springer: New York, 1990; Appendix F. Also: Gutowsky, H. S.; Holm, C. H. *J. Chem. Phys.* **1957**, *25*, 1288. Kaplan and Fraenkel discuss the spectrum of dimethylformamide-d_1. The presence of the amide hydrogen causes spin–spin coupling which complicates the interpretation. See: Rabinovitz, M.; Pines, A. *J. Am. Chem. Soc.* **1969**, *91*, 1585.

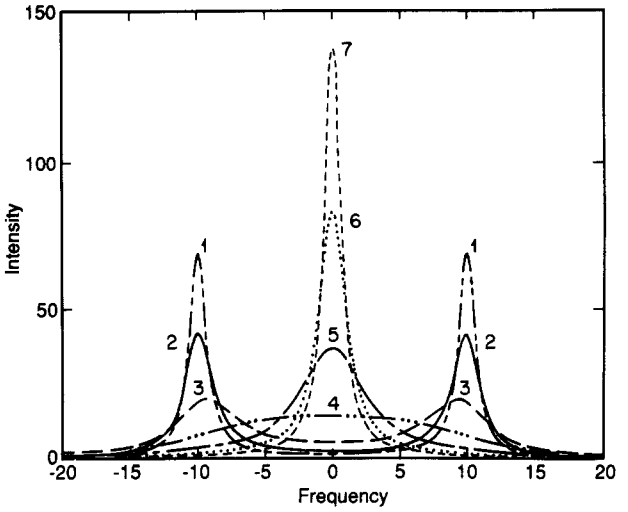

Figure 2. Theoretical magnetic resonance spectra for a collapsing pair of lines such as brought about by the mechanism of Figure 1. The spectra are plotted for different values of the Kubo parameter $\kappa = \Delta\tau$, where 2Δ is the frequency separation for no exchange and τ is the reciprocal rate of reaction. Δ is taken as 10 units, spectrum 1 is for $\kappa = 31$, and the other spectra are for progressively smaller κ. Note that if the splitting of the lines is 20 rad/s, or $20/2\pi = 3$ Hz, then τ for the widest line, 4, would be 1/10 s.

an increase in the chemical exchange rate induces a *broadening* and *shifting toward one another* of the spectral lines resulting from individual sites, while once band collapse has occurred, for $\kappa \ll 1$, any further increase in the exchange rate leads to a *narrowing* of the single band. The time scale which determines whether the chemical exchange is "slow" or "fast", and thus the details of the effect of the exchange on the band profile, is set by the inverse of the modulation amplitude Δ^{-1}.

It should be noted that the exchange process of Figure 1 assumes implicitly that the exchange is instantaneous, i.e., very fast compared to Δ^{-1}. The crucial transition time, τ_t, turns out to be in the approximate range 0.1–1.0 ps for condensed-phase systems. Since for most NMR experiments Δ^{-1} is in the range 10^{-3}–1.0 s, that is, $\Delta/2\pi$ is in the range of hertz to kilohertz, the condition $\tau_t \ll \Delta^{-1}$ is fulfilled very well. This will *not* turn out to be true for chemically exchanging *vibrational* systems.

IV. Vibrational Spectra

One-Well Vibrational Systems: Hot Bands and the "Exchange" Model. There is another situation in which Figure 1 is applicable. That is where only the four quantum states characterize the system and there is a rate process that exchanges the two sets of two. Under these circumstances, there are no intermediate states and the simple exchange picture is applicable. This is the situation for the interaction of a vibrational fundamental with its "hot band" in the limit of low temperature. In this case, the wavy line signifies the $0 \rightarrow 1$ transition of a vibrational mode, such as that of a stretch or bend that might be observed in a Raman or infrared experiment. The anharmonic coupling between the high-frequency mode (with coordinate q) and a lower frequency mode (with coordinate Q) shifts the energy levels of the high-frequency mode, so that its transition frequency depends on the number of quanta n_Q in the low-frequency mode. The exchange of quanta between the low-frequency mode and other "bath" degrees of freedom therefore modulates the vibrational frequency being probed. The resulting "exchange dephasing" is described by the theory of Harris et al.[5,6] The expression "exchange" was originally applied to situations in which pairs of spins flip together.[7] Here, it is taken over to any analogous process involving four levels. At low temperatures,

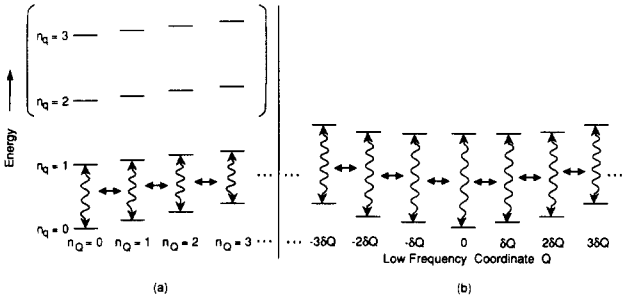

Figure 3. Exchange between a vibrational fundamental and its hot bands, due to anharmonic coupling. The high-frequency (experimentally observed) mode has coordinate q; the low-frequency mode, which exchanges energy with the bath and also is coupled to the high-frequency mode, has coordinate Q. (a) The low-frequency mode is treated quantum mechanically. The vibrational quantum numbers are n_q and n_Q. The states in parentheses, having at least two quanta in the high-frequency mode, may be neglected in most cases, as long as $\hbar\omega_q \gg kT$. (b) The low-frequency mode is treated classically as a function of its position Q. The probe frequency ω_q follows Q adiabatically. The resulting low-frequency potential wells for $n_q = 0$ and $n_q = 1$ are divided into small pieces of width δQ, so that Q motion is described by jumps between adjacent positions, as represented by the arrows.

when there is at most only one quantum of energy in the low-frequency mode, the "two-site" picture of Figure 1 describes the system well. The bulk of the intensity will be in the $n_Q = 0$ fundamental band (the A states in Figure 1), and as the exchange rate increases with increasing temperature, this band will broaden and shift. The $n_Q = 1$ hot band (B states) also becomes more intense as the temperature increases.

At higher temperatures, the entire picture changes because the whole manifold of low-frequency quantum states must be considered, as illustrated in Figure 3a.

Note that, although the same energy level diagrams describe chemical exchange in NMR and hot band "exchange dephasing" in vibrational spectra, the two kinds of exchange involved are physically very different. The NMR chemical exchange is an exchange between physical sites, whereas the vibrational exchange dephasing is simply an exchange of levels *in the same site*, due to the addition or subtraction of a quantum of energy.

For high enough temperatures, where the quantum coherence of the low-temperature mode is significantly perturbed by thermal fluctuations in the bath to which it is coupled, it is often preferable to describe the low-frequency motion classically. Then the dynamics of the low-frequency mode can be modeled by using the techniques of classical statistical mechanics. One tractable approach[8] models the dynamics as an Ornstein–Uhlenbeck process. This process[9] is a damped harmonic oscillator driven by a random force, that is

$$\ddot{Q} + \beta\dot{Q} + \omega_Q^2 = f(t)/m \tag{12}$$

where Q is the coordinate of the low-frequency motion, ω_Q its frequency in the absence of damping, m its reduced mass, β the damping constant, and $f(t)$ a random force such as that a solvent might exert on a heavy particle undergoing Brownian motion. However, the low-frequency dynamics of real systems may also be different than this, and other approaches to the dynamics are possible.[10]

The anharmonic coupling between the low- and high-frequency modes arises from coupling terms in the Hamiltonian such as

$$H' = k'Qq^2 \tag{13}$$

and

$$H'' = k''Q^2q^2 \tag{14}$$

(5) Harris, C. M.; Shelby, R. M.; Cornelius, P. A. *Phys. Rev. Lett.* **1977**, *38*, 1415. Shelby, R. M.; Harris, C. B.; Cornelius, P. A. *J. Chem. Phys.* **1979**, *70*, 34.
(6) Nitzan, A.; Persson, B. W. J. *J. Chem. Phys.* **1985**, *83*, 5610.
(7) Skinner, J. L.; Hsu, D. *J. Phys. Chem.* **1986**, *90*, 4931.
(8) Robertson, G. N.; Yarwood, J. *Chem. Phys.* **1978**, *32*, 267–282.
(9) Uhlenbeck, G. E.; Ornstein, L. S. *Phys. Rev.* **1930**, *36*, 823. Reprinted in: Wax, N., Ed. *Selected Papers on Noise and Stochastic Processes*; Dover: New York, 1954; p 113.
(10) Johnson, W. G.; Oxtoby, D. W. *J. Chem. Phys.* **1987**, *87*, 781.

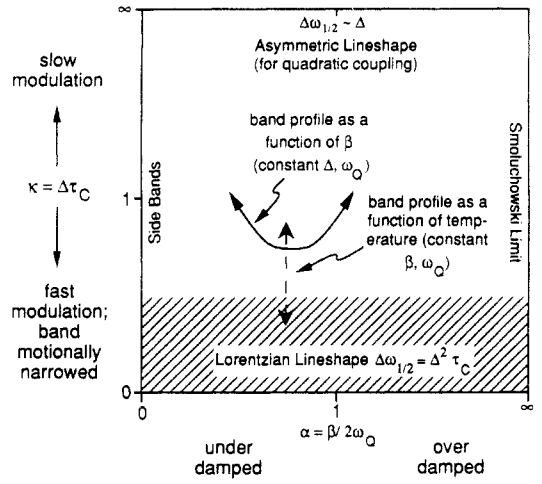

Figure 4. Characterization of the band profile arising from exchange coupling as a function of the dimensionless Kubo and damping parameters κ and α. We call this a "Kubo" diagram. The solid and dashed lines show how the band profile parameters change when the damping constant β or the temperature is changed, while holding other parameters constant, for the case of a *quadratic* coupling (eq 14). For quadratic coupling, $\tau_c = {}^1/_2(\beta^{-1} + \beta/\omega_Q^2) = (1/\omega_Q)(\alpha + 1/4\alpha)$ and $\Delta \propto T$. The cross-hatched area indicates the approximate region for which nonperturbative results for the bandwidth have been obtained.[6,7]

As the low-frequency mode coordinate Q varies with time, these coupling terms produce a stochastic modulation of the higher frequency. Generally, the coupling term linear in Q (eq 13) would be expected to give the dominant contribution to the dephasing, unless this term is absent because of symmetry constraints or the Q motion has a very large amplitude.[7,11-14] If the low-frequency mode is modeled as an Ornstein–Uhlenbeck process, eq 12, its dynamics can be characterized by the dimensionless damping parameter $\alpha = \beta/2\omega_Q$. The motion is overdamped for $\alpha > 1$ and underdamped for $\alpha < 1$. Then for a given form of the anharmonic coupling, the band profile can be characterized as a function of two parameters, α and the Kubo parameter κ. This is illustrated in Figure 4 for the case of a quadratic coupling. The diagram, which we call a *Kubo diagram*, is not simple for this coupling. Depending on the values of the parameters, one can have motionally collapsed Lorentzian or non-Lorentzian lines, sidebands or a single band, and so on.

For a specific form of the anharmonic coupling, the band profile may be characterized as a function of a given parameter, such as temperature or damping constant, by a curve on the α–κ plane. For the quadratic coupling of Figure 4, $\tau_c = {}^1/_2(\beta^{-1} + \beta/\omega_Q^2) = 1/\omega_Q(\alpha + {}^1/_4\alpha)$,[12,13] and the Kubo parameter has a minimum as a function of β. This occurs when $\alpha = \beta/2\omega_Q = {}^1/_2$ for fixed values of Δ and ω_Q. Thus, as the diagram indicates, motional narrowing *cannot* be attained for a quadratic coupling in the strongly overdamped and underdamped limits, but only (if at all) for a range of damping parameter values around $\alpha = {}^1/_2$. This is in contrast to the linear coupling case, where $\tau_c = \beta/\omega_Q^2$ and the band is always motionally narrowed in the underdamped limit.

An energy level diagram analogous to Figure 3a can be drawn for the case of a classical low-frequency mode, by discretizing the low-frequency coordinate Q in steps of δQ. This is shown in Figure 3b. Such a picture is of limited utility in the case of underdamped Q motion, since then the Q motion is periodic and the "exchange" between different Q locations is very rapid. In the case of overdamped Q motion, on the other hand, the system executes a slow diffusion between different Q "sites", with an effective diffusion time constant β/ω_Q^2. Then the picture of Figure 3b is very useful.

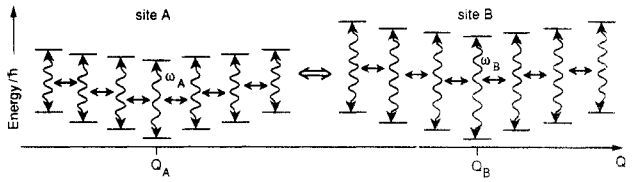

Figure 5. A picture of chemically exchanging vibrational bands in the limit of instantaneous jumps between sites. Unlike the case of NMR chemical exchanges (Figure 1), here each site contains a manifold of states with many degrees of freedom. For each site, only one of the low-frequency degrees of freedom is shown, namely, that motion along the reaction coordinate Q. The frequencies ω_A and ω_B are the probe vibrational frequencies for the well potential minima Q_A and Q_B; elsewhere in the wells the frequency will differ somewhat due to anharmonic coupling.

We note that, in this strongly overdamped limit, the dynamics of the Q motion can be described by the simple Smoluchowski equation, rather than the more complicated Fokker–Planck equation. The Fokker–Planck equation treats inertial effects explicitly and describes the Ornstein–Uhlenbeck process for any value of the damping constant α. The Smoluchowski equation is a simplified version of the full Fokker–Planck equation, which does not contain the kinetic energy and is appropriate for highly damped motion ($\alpha \gg 1$).

Chemical Exchange in Vibrational Spectroscopy. We are now in a position to describe the effect of chemical exchange on vibrational spectra and emphasize the differences between chemical exchange in vibrational spectroscopy and in the more familiar NMR case. The first difference between the two kinds of chemical exchange is evident from comparing an NMR "site", which is a two-level system such as each of the pair of states in Figure 1, with a vibrational "site" such as is typified in Figure 3. Chemical exchange in NMR is exchange between pairs of states, while for vibrational spectra exchange occurs between *manifolds* of states. A diagram symbolizing chemical exchange in vibrational spectroscopy, analogous to the NMR case of Figure 1, might take the form of Figure 5. In this figure, the only low-frequency motion considered is that along the reaction coordinate Q (but within the wells of the two sites A and B). In general, of course, there will also be other low-frequency modes that couple anharmonically to the high-frequency vibration, which will lead to further exchange dephasing. In many cases, however, these other couplings may be rapidly modulated and their contribution to the overall vibrational bandwidth can be accounted for simply by adding an extra dephasing line width $1/T_2'$, which can be convoluted with the rest of the spectrum.[2]

Depicting the chemical exchange process as an instantaneous jump, as in Figure 5, is valid when the transit time between sites $\tau_t \ll \Delta^{-1}$, just as in the NMR case. Such an approximation is implicitly made when using the Bloch equation approach to chemical exchange. As we have emphasized previously,[2,13] however, in vibrational spectroscopy it is difficult to fulfill the $\tau_t \ll \Delta^{-1}$ condition. For vibrational spectra a typical value of Δ is on the order of 10 cm^{-1} which is equivalent to 2×10^{12} s^{-1}, so that the jump between manifolds must take place in a time $\tau_t \ll 5 \times 10^{-13}$ s for the condition $\tau_t \ll \Delta^{-1}$ to be valid. This is a nearly impossible condition, as we shall now see.

Perhaps the simplest model useful for estimating a time scale is for a free particle with an energy determined by the temperature. Then the velocity for one-dimensional motion can be determined by equating the thermal and kinetic energies:

$$ {}^1/_2kT = {}^1/_3mv^2 \qquad (15) $$

If we take $T = 300$ K and $m = 30$ amu, we can find the average velocity. If the distance between sites is 1 Å, the transit time, τ_t, is 0.3 ps. This is the fastest reasonable time at room temperature. A more realistic estimate that takes account of hindering forces is an estimate from the one-dimensional diffusion equation

$$ d^2 = 2Dt \qquad (16) $$

where d is the distance traveled and D is the diffusion constant.

(11) Persson, B. N. J.; Ryberg, R. *Phys. Rev.* **1985**, *B32*, 3586.
(12) MacPhail, R. A.; Snyder, R. G. *J. Chem. Phys.* **1989**, *91*, 3895.
(13) Wood, K. A.; Snyder, R. G.; Strauss, H. L. *J. Chem. Phys.* **1989**, *91*, 5255.
(14) MacPhail, R. A.; Snyder, R. G.; Strauss, H. L. *J. Chem. Phys.* **1982**, *77*, 1118.

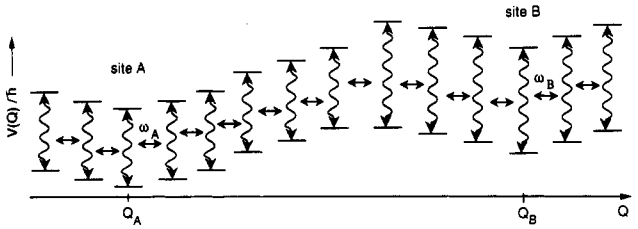

Figure 6. A more complete picture of the vibrational bands during chemical exchange, which includes the transition barrier region. Compare to Figure 5. The barrier region must be considered because motion along the reaction coordinate Q is slow.

D has a value of 10^{-5} cm^2/s in most room-temperature liquids, and this gives $\tau_t = 5$ ps for an excursion of 1 Å. Some reactions may tunnel, and it is interesting to ask for the transit time for this process. Such a time has been estimated,[2,15] and the time can be rapid for tunneling well below the top of the barrier. For this rapid time, however, the rate of reaction, τ^{-1}, is small and the reaction has no effect on the spectrum.

In summary then, the transit time for a typical room-temperature reaction is just about the same as the reciprocal of a typical spectral splitting. This means that, although a reaction can modify the spectrum, the effect of the reaction is mixed together with that of other relaxation processes, and we must understand these processes in order to determine the reaction rate.

We have already noted that band collapse occurs when the Kubo parameter $\kappa = \Delta\tau_c$ is on the order of one. For systems exhibiting exchange collapse, τ_c is simply a measure of the average time the system spends in a site between exchange events (eq 11). For chemically exchanging vibrational bands, then, in the limit of rapid exchange, the time spent in each potential well will become comparable to the time spent crossing the barrier. The lack of a good time scale separation between τ_t and τ_c (and between τ_t and Δ^{-1}) makes it necessary to consider the details of the barrier-crossing process. In the limit of diffusive motion, this can be symbolized by replacing the picture of Figure 5 by one such as Figure 6. Here the site-exchange arrow has been replaced by a manifold of states representing the barrier-crossing process. In such a picture, there is no longer a clean separation between reactive and nonreactive motions. In such situations, a Bloch equation or site model treatment is problematic; it becomes necessary to model the entire Q (reaction) coordinate dynamics explicitly and also treat explicitly the dependence of the vibration (q) frequency on Q in both the barrier and the well regions.[2,16]

Figure 7 shows a typical effective potential function for a two-well system, and the resulting probability distribution, as a function of the reaction coordinate Q for a temperature at which the A ↔ B exchange process is slow. Also shown is one way in which the vibrational frequency ω varies with Q. For the sake of simplicity, $\omega(Q)$ is drawn as a monotonic function, but it need not be monotonic for all physical systems. Now consider two types of motion in the Q coordinate: (1) nonreactive *within* each well, the intrawell motion, and (2) reactive motion between the two wells, the interwell motion. Assuming that the reactive and nonreactive motions can be approximately separated, each type of motion can be characterized by modulation parameters. For the *reactive* motion, in analogy to eq 11, we define

$$\Delta_{rxn} \equiv |\omega_B - \omega_A|/2$$

$$\tau_c^{rxn} \equiv \tau_{rxn}/2$$

$$\kappa_{rxn} \equiv \Delta_{rxn}\tau_c^{rxn} \qquad (17)$$

so that κ_{rxn} is a dimensionless Kubo parameter characterizing the degree of band collapse due to chemical exchange. For the nonreactive intrawell motion, the probability distribution $P(Q)$ yields a mean-square displacement of the system within the well

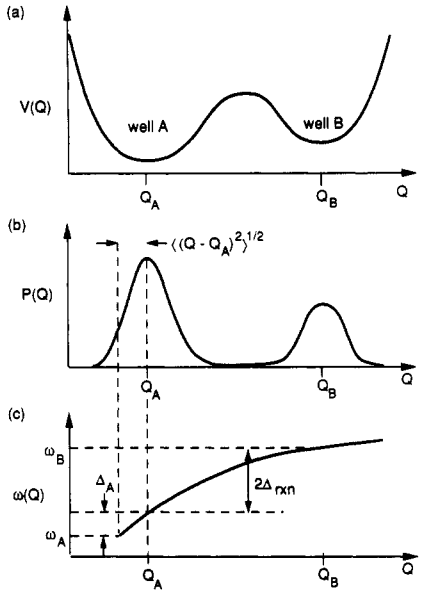

Figure 7. Approximate potential function (a), probability distribution (b), and vibrational frequency, $\omega_q(Q)$ (c), of a two-site system, as a function of the reaction coordinate Q, for the case where the vibrational frequency $\omega(Q)$ increases monotonically. Also indicated is the change of frequency Δ_A due to motion in the A well and the change Δ_{rxn} due to the motion between wells.

$(\Delta Q_A)_{rms} \equiv [\langle (Q - Q_A)^2 \rangle_A]^{1/2}$, where $\langle\ \rangle_A$ denotes an average over the probability distribution in the A well. Then the modulation parameters for the A well are on the order of

$$\Delta_A \equiv |(\partial\omega/\partial Q)_{Q=Q_A}|(\Delta Q_A)_{rms}$$

$$\tau_c^A = \beta(\omega_Q^A)^2 \equiv 2\alpha\omega_Q^A$$

$$\kappa_A = \Delta_A\tau_c^A \qquad (18)$$

where the superscript A refers to the A well. Here ω_Q^A is the harmonic frequency for the Q motion in the A well, α and β are damping parameters for this motion, and the expression for τ_c is that appropriate for an effective coupling which is linear in Q, i.e., $\omega = \omega_A + (\partial\omega/\partial Q)Q$ (the situation shown in Figure 7). A similar set of quantities characterize the motion in the B well.

To characterize the band profile of this kind of chemically exchanging system, *at least* three dimensionless parameters are needed: the damping parameter α, κ_A, which characterizes the intrawell dynamics, and κ_{rxn}, which characterizes the rate of the reaction. These parameters define a three-dimensional space. If, however, it is assumed that the damping parameter α is constant for all temperatures and all values of Q and that the modulation parameters of wells A and B are similar [note that this need not be true, e.g., in Figure 7c, $\omega(q)$ is such that $\Delta_A > \Delta_B$], then a two-dimensional characterization of the band profile is possible, using κ_A and κ_{rxn}. This is shown in Figure 8. The behavior of the band profile as a function of temperature for two different low-temperature values of Δ_A is shown by the solid and dashed curves. To obtain these curves, it is assumed that: Δ_{rxn} is constant; the reaction rate $(\tau_c^{rxn})^{-1}$ increases in Arrhenius fashion; $\Delta_A \propto T^{1/2}$ but $\Delta_A < \Delta_{rxn}$ always (in accord with Figure 7c); τ_c^A = constant $\ll (\tau_c^{rxn})$ (low T); $\tau_c^A \leq \tau_c^{rxn}$ (high T). This means that the intrawell modulation rate $(\tau_A^A)^{-1}$ is always at least as fast as the interwell rate $(\tau_c^{rxn})^{-1}$. Then $\kappa_A \leq \kappa_{rxn}$ at all temperatures. Note that, as we have mentioned repeatedly, κ_{rxn} cannot go much less than one for vibrational spectra, and therefore the left-hand side of the Kubo diagram corresponds to impossible situations.

The curves in Figure 8 are for the case where $\omega(Q)$ is monotonic. Other situations are also possible, as shown in Figure 9, which applies, for instance, to the C–H stretching mode of cyclopentane for which the stretching frequency as a function of the molecular pseudorotation angle can be accurately calculated.[17] For a case

(15) Buttiker, M.; Landauer, R. *Phys. Rev. Lett.* **1982**, *49*, 1739. See also: Hauge, E. H.; Stouneng, J. A. *Rev. Mod. Phys.* **1989**, *61*, 917.
(16) Cavagnat, D.; Lascombe, J. *J. Chem. Phys.* **1982**, *76*, 4336.
(17) MacPhail, R. A.; Variyar, J. E. *Chem. Phys. Lett.* **1989**, *161*, 239.

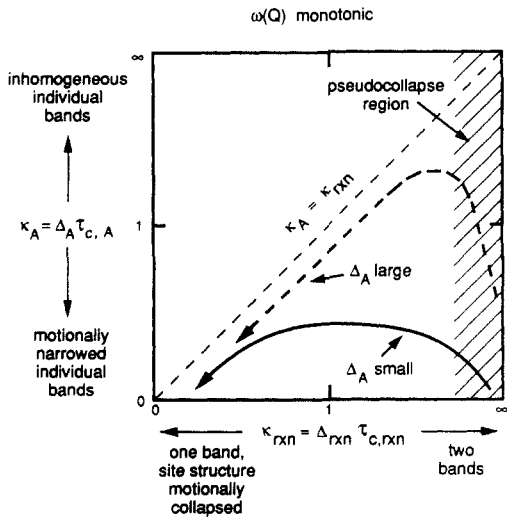

Figure 8. A Kubo diagram showing how the Kubo parameters κ_A and κ_{rxn} might change as a function of temperature, for a pair of chemically exchanging vibrational bands. The two curves correspond to different low-temperature values of Δ_A. It is assumed that $\omega(Q)$ is monotonic and therefore that $\Delta_{rxn} > \Delta_A$; see Figure 7c. Note that there are two correlation times: $\tau_{c,A}$ the intrawell (nonreactive) time and $\tau_{c,rxn}$ the interwell (reaction) time. "Pseudocollapse" occurs for large values of κ_{rxn}, as indicated by the shaded region. Since $\tau_{c,rxn}$ cannot be very small for the reactions we consider, the part of the diagram on the extreme left does not correspond to physically realizable situations.

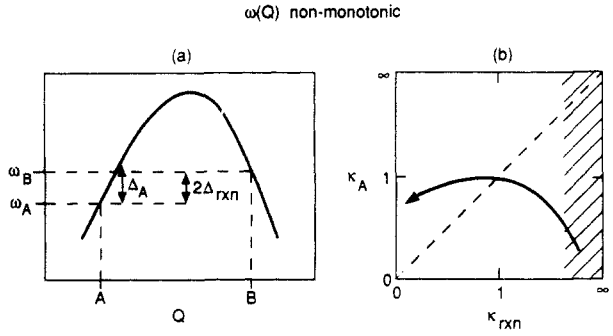

Figure 9. Variation of the frequency $\omega_q(Q)$ and the Kubo diagram for a two-well system, as in Figure 7a,b, but for a nonmonotonic frequency variation. Note that here Δ_A can be greater than Δ_{rxn} at high temperature, unlike the case of Figure 8, and the Kubo diagram changes as a result.

such as this, it is no longer always true that $\Delta_A < \Delta_{rxn}$, and the Kubo parameter κ_A need not tend to zero for fast reaction rates. For such systems, motional narrowing can be incomplete even for the fastest chemical exchange rates.

Another possible situation occurs when $V(Q)$ and $\omega(Q)$ are periodic, such as might occur when the reaction coordinate is a reorientation about some symmetry axis in the solid state. One example is the rotation of *n*-alkanes in the hexagonal channels of urea clathrates.[13,18] This situation is shown in Figure 10. Here the sites are equivalent so that $\Delta_{rxn} = 0$, and no band collapse can occur, only band broadening. Part of this broadening can be due to hopping between wells; the rest of it will be due to other mechanisms such as exchange coupling with the intrawell Q motion. For the latter kind of exchange coupling, we note that the coupling is necessarily quadratic in Q due to the symmetry of the well (eq 14), and this causes a temperature-dependent shift in the band frequency.[13]

Pseudocollapse and the Mechanisms of Band Broadening. We have already noted that an increase in the rate of chemical exchange (e.g., due to a change in temperature) can lead to either band *broadening* (in the slow modulation, i.e., two-band limit)

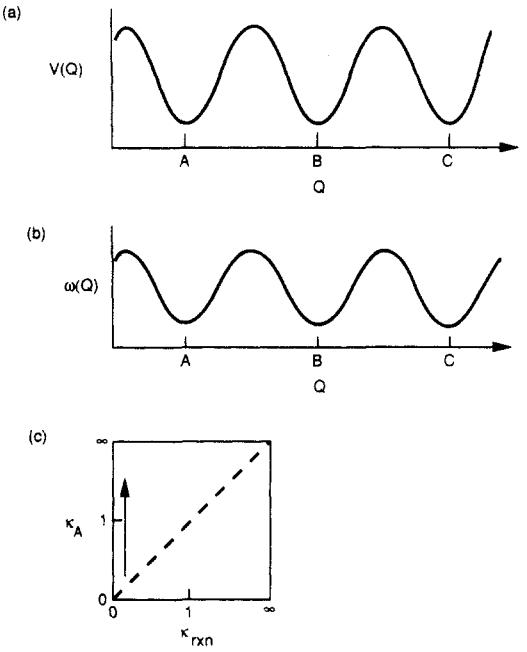

Figure 10. Potential, vibrational frequency, and resulting Kubo parameter diagram for the case of exchange between multiple equivalent sites. Here, Q can, for example, correspond to the rotation of a molecule about a symmetry axis in a crystal. Then $\Delta_{rxn} = 0$, and consequently there is only one band, the width of which changes with the parameters.

or band *narrowing* (in the fast modulation, i.e., collapsed multiplet limit). It often happens experimentally that the chemical exchange rate cannot be varied over a range wide enough to see the complete exchange collapse of well-separated vibrational bands. In such cases, the chemical exchange rate has sometimes been inferred by studying the early stages of collapse, i.e., the broadening and moving together of bands as a function of increasing temperature. However, it is obvious from the earlier parts of this paper that many other mechanisms can also contribute to line shifts and increased widths for the same band. In particular, exchange modulation of the vibrational frequency due to *intrawell* motions along the reaction coordinate will in general give rise to an apparent broadening and shifting of the vibrational bands that is totally unrelated to the chemical exchange rate. This apparent collapse, which we will call *pseudocollapse*, was identified by Corn and Strauss[19] and Cavagnat and Lascombe.[16] It has since been identified in a number of other systems.[20-23]

Pseudocollapse is easily demonstrated through numerical simulations. Figure 11 shows the vibrational band profile in the slow modulation limit for a symmetric double-well potential of the form $U(Q) = AQ^8 - BQ^2$. This form of the potential function gives a double well with very steep outer walls: a form, which at low excitation energies, is nearly a square well with a hill in the middle. The probe vibrational frequency is assumed to be a linear function of Q. Then the vibrational envelope simply mirrors the probability distribution that the system will be found at a given value of Q. This distribution is always peaked at the potential minimum positions. However, due to the anharmonicity, which will normally be appreciable in reacting systems, the first moments (average frequencies) of the bands shift inward. At the same time, the bands broaden with increasing temperature.

If these bands are motionally narrowed, with a correlation time that is independent of temperature, one obtains the pseudocollapse

(18) Cho, Y.; Kobayashi, M.; Tadokoro, H. *J. Chem. Phys.* **1986**, *84*, 4643.

(19) Corn, R. M.; Strauss, H. L. *J. Chem. Phys.* **1982**, *76*, 4834.

(20) Besnard, M.; del Campo, N.; Lascombe, J. In *Chemical Reactivity in Liquids. Fundamental Aspects*; Moreau, M., Turq, P., Eds.; Plenum: New York, 1988; p 33.

(21) Sension, R. J.; Strauss, H. L. *J. Chem. Phys.* **1987**, *86*, 6665.

(22) Hayden, B. E.; Bradshaw, A. M. *Surf. Sci.* **1983**, *125*, 787.

(23) Jones, T. S.; Holloway, S.; Gadzuk, J. W. *Surf. Sci.* **1987**, *184*, L421.

TABLE I

case	figure	dependence of $\omega(Q)$ on Q in rxn region	relation[a] of Δ_{rxn}, Δ_A	pseudocollapse behavior behavior with increasing rate	in principle result of fast chemical exchange
I. $\omega(Q)$ monotonic	6, 7	linear	$\Delta_{rxn} > \Delta_A$	bands broaden, shift together somewhat (Figure 11)	full band collapse and narrowing
II. $\omega(Q)$ parabolic	8	linear	$\Delta_{rxn} \leq \Delta_A$ at high temps	bands broaden (may merge); shift in same direction	full band collapse and narrowing
III. $V(Q)$, $\omega(Q)$ periodic	9	quadratic	$\Delta_{rxn} = 0$	single band broadens; shifts with temperature	single band broadening, then narrowing for fastest reaction rates

[a] Δ_{rxn} is the change of frequency between sites; Δ_A is the intrawell change of frequency.

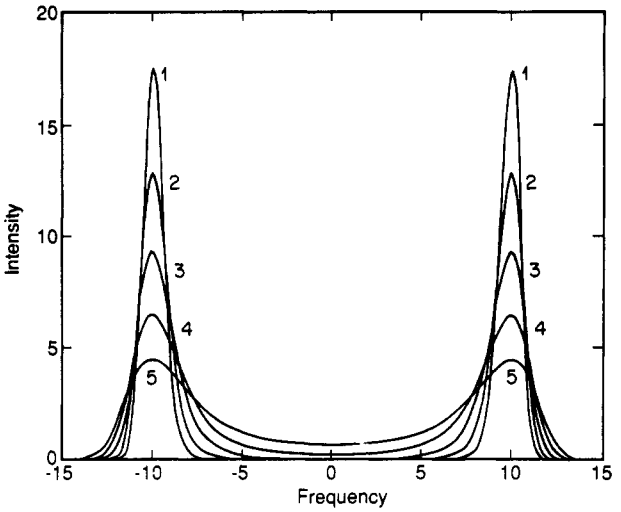

Figure 11. Vibrational band profiles of a doublet in the slow modulation limit, i.e., for $\tau_{c,A} = \infty$ (also $\tau_{c,rxn} = \infty$). The potential is of the form $V(Q) = AQ^8 - BQ^2$. The vibrational frequency is taken as linear with respect to Q, with the proportionality constant adjusted such that $\omega_A = \omega_0 - 10$, $\omega_B = \omega_0 + 10$ in arbitrary frequency units. The zero of frequency, ω_0, on this scale corresponds to the average frequency. The band profiles are noted for a number of values of U/kT, where U is the barrier height and T the absolute temperature. Spectrum 1 is for the lowest temperature, and the successive spectra are for increasing temperature. For spectrum 5, $U/kT = 2$. In this slow modulation limit, the band profile simply reflects the population distribution, weighted according to the Boltzmann factor, as a function of Q.

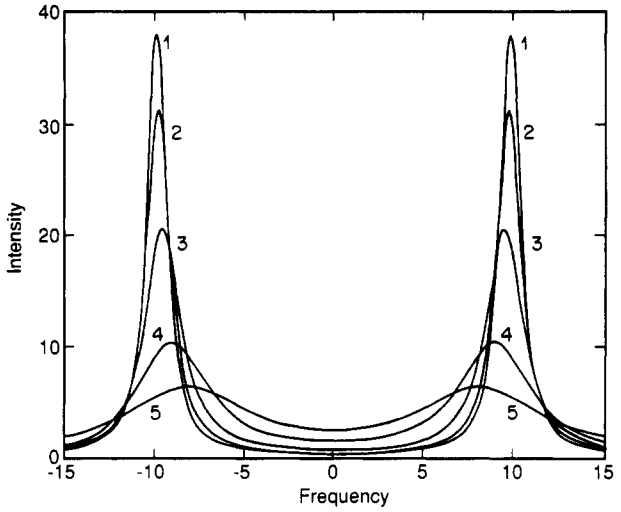

Figure 12. Vibrational band profiles of the doublet of Figure 11, where the band in each well (separately!) is motionally narrowed into a Lorentzian centered at the average frequency of the slow modulation band, with hwhh $\Gamma = \Delta^2\tau_{c,A} + \Gamma_{residual}$, where $\tau_{c,A}$ is taken arbitrarily as 0.106 so that $\kappa_A \leq 1$ for all temperatures, Δ^2 is the second moment of the band in the slow modulation limit (see text), and the residual bandwidth $\Gamma_{residual}$, which takes into account intrawell relaxation mechanisms that do not involve motion along the reaction coordinate, is $\Gamma_{residual} = 2$. As with Figure 11, U/kT is the ratio of the barrier height to the temperature. The site-exchange (reaction) rate is still zero ($\tau_{c,rxn} = \infty$), so that the "collapse" behavior of the lines is the result of the anharmonicity of the potential well and the linear dependence of the frequency on the reaction coordinate and is not due to chemical exchange.

spectrum of Figure 12. Here, band broadening and shifts are observed, just as for the case of chemical exchange. However, this pseudocollapse is independent of the reaction rate, a rate that has not even been included in the above calculations and that can be much slower than the rate processes we have included.

Pseudocollapse was identified at low temperatures in a crystal[19] by noting that the low-temperature changes in the band profiles were much greater than those expected from an extrapolation of the Arrhenius-type behavior observed at higher temperatures. Many systems, however, cannot be probed or characterized over a temperature range wide enough to unambiguously demonstrate deviations from Arrhenius behavior. In such cases, it can be difficult to say whether chemical exchange processes contribute to the band shifts and broadening or instead that the spectral changes are due simply to some sort of pseudocollapse mechanism. The two mechanisms can be separated if the variation in the band can be observed over the entire range of κ (Table I), but few vibrational systems allow this.

Pseudocollapse is relevant to systems for which the vibrational frequency varies monotonically with the reaction coordinate, as in Figures 7 and 8. For other situations, such as those shown in Figures 9 and 10, the relative magnitudes of the band shifts and band broadenings will differ. The behavior of the band profiles for the different kinds of systems and the contrast between pseudocollapse and fast reaction behavior is summarized in Table I.

Figure 13 shows the pseudocollapse at low temperatures and combination of pseudocollapse and collapse at high temperatures thought to occur for the water molecule HOD in $NaClO_4 \cdot H_2O$.[19]

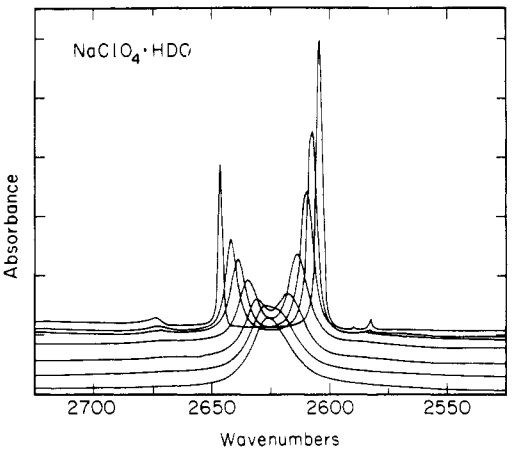

Figure 13. Infrared band collapse of the O–D stretching band of lightly deuterated $NaClO_4 \cdot H_2O$ from ref 19. The spectra are at 10, 70, 100, 175, 200, 250, and 290 K. The two hydrogens of the water molecule are at inequivalent sites in the crystal, leading to two O–D stretch infrared lines at low temperature. The spectra at 100 K and below show pseudocollapse from processes unrelated to the site-exchange process that exchanges the two water hydrogens, as in Figure 11. At higher temperatures, the site-exchange process becomes fast enough to affect the spectra, and true band collapse occurs together with pseudocollapse.

This set of spectra illustrates the combination of relaxation processes that contribute to observed band merger.

V. Conclusions

The bottom line is that due to the vastly different time scales of magnetic resonance and vibrational spectroscopies, the details of the applicable relaxation processes are very different. In particular, for an ordinary room-temperature thermal reaction involving motion of the nuclei, the reaction rate *cannot* be simply deduced from changes in the vibrational spectra. This is true even if the changes in the vibrational spectra look very much like those that characterize the magnetic resonance spectra of reacting systems.

Our argument states that, for systems that react fast enough to affect a condensed-phase vibrational spectrum, the transit time must be of the same magnitude as the other times in the problem or even longer. Therefore, details of the observed frequency $\omega_q(Q)$ in the transition region become important. The methods used to analyze the spectra must take into account this functional dependence. Correct methods for taking into account reactions usually involve calculating correlation functions of the frequency under a variety of assumptions.

In this review, we have illustrated the possible behavior of vibrational bands as a function of the various times in a series of "Kubo diagrams". These diagrams have been drawn qualitatively for different possible forms of $\omega(Q)$ and are given in Figures 4, 8, 9, and 10.

There have been numerous attempts to analyze the spectra of reacting systems. A more technical review both of the theory and of various applications—right and wrong—may be found in a further review.[24] Some successful applications of the theory to actual spectra are found in the literature: for example, the motion of water in $NaClO_4 \cdot H_2O$,[19] the motion of a methyl group of an alkane chain,[14] and the rotation–torsion of methylene groups of an alkane.[13] The first of the three examples illustrates a linear dependence of ω on Q, while the other two illustrate quadratic dependencies.

Finally, we note that although we have shown that the relationship between the broadening and shifts of vibrational bands and thermal chemical reaction rates is complex, it might be possible to use new techniques of vibrational spectroscopy to determine these rates. The different techniques, for example, resonance Raman, two color, and time-domain spectroscopies, are sensitive to different relaxation processes. New experiments using these techniques to measure thermal reaction rates can probably be designed.

Acknowledgment. We particularly thank Professor Richard A. MacPhail for helpful discussions. We thank the National Science Foundation (CHE 88-14565) and the National Institutes of Health (GM27690) for support.

(24) Wood, K. A.; Strauss, H. L. *Int. Rev. Phys. Chem.*, to be published.

ARTICLES

Picosecond Ground-State Rotational Diffusion of Merocyanine 540 in Polar Solvents

Edward L. Quitevis* and Miin-Liang Horng

Department of Chemistry and Biochemistry, Texas Tech University, Lubbock, Texas 79409
(Received: July 18, 1989; In Final Form: February 8, 1990)

The ground-state rotational diffusion of merocyanine 540 in polar solvents was studied by using picosecond polarized transient bleaching. The rotational diffusion time τ_{rot} was obtained from fits of a single exponential to the absorption anisotropy. The value of τ_{rot} was 78 ± 5 ps in acetone, 130 ± 24 ps in methanol, 190 ± 19 ps in dimethylformamide, 270 ± 30 ps in ethanol, 490 ± 50 ps in 1-propanol, 530 ± 13 ps in dimethyl sulfoxide, and 700 ± 130 ps in 1-butanol. The dependence of the observed rotational diffusion time on the solvent's shear viscosity was the same in protic and aprotic solvents. The reorientational dynamics of this dye in these solvents can be explained by hydrodynamics for a prolate ellipsoid using stick boundary conditions. The absence of effects due to hydrogen bonding and dielectric friction in alcohol solvents is discussed.

Introduction

Merocyanine 540 (MC 540) (Figure 1) is a lipophilic polymethine dye that binds to biological and synthetic membranes. MC 540 has well-characterized spectral and binding properties in homogeneous solutions,[1] SDS micelles,[2] phosphatidylcholine vesicles,[3,4] and mitochondria.[4] Although MC 540 is negatively charged, it binds to anionic micelles.[2] The driving force of the binding is due to the hydrophobic interactions of the two tetramethylenic tails of the molecule, which become embedded within the membrane. The excited-state properties of MC 540 are sensitive to electrical potential, and its fluorescence has been used to probe the transmembrane potential of many cell and organelle membranes.[5] There has been growing interest in exploiting the differential affinity and selective phototoxicity of MC 540 for biomedical applications.[6-8] In order to unravel the photodynamics of MC 540 in these complex biological systems, it is necessary to probe the dye's local membrane environment. Rotational diffusion is an ideal probe, because it is sensitive to membrane order and rigidity.[9] However, the dye's reorientational dynamics

(1) (a) Dixit, N. S.; Mackay, R. A. *J. Am. Chem. Soc.* **1983**, *105*, 2928. (b) Aramendia, P. F.; Krieg, M.; Nitsch, C.; Bittersmann, E.; Braslavsky, S. E. *Photochem. Photobiol.* **1988**, *48*, 187.
(2) Dodin, G.; Aubard, J.; Falque, D. *J. Phys. Chem.* **1987**, *91*, 1166.
(3) Verkman, A. S.; Frosch, M. P. *Biochemistry* **1985**, *24*, 7117. (b) Verkman, V. S. *Biochemistry* **1987**, *26*, 4050.
(4) (a) Dodin, G.; Dupont, J. *J. Phys. Chem.* **1987**, *91*, 6322.
(5) Waggoner, A. S.; Grinvald, A. *Ann. N.Y. Acad. Sci.* **1977**, *303*, 217.
(6) Sieber, F. *Photochem. Photobiol.* **1987**, *46*, 1035.
(7) Sieber, F.; Spivak, J. L.; Sutcliffe, A. M. *Proc. Natl. Acad. Sci. U.S.A.* **1984**, *81*, 7584.
(8) Sieber, F.; O'Brien, J. M.; Krueger, G. J.; Schober, S. L.; Burns, W. H.; Sharkis, S. J.; Sensenbrenner, L. L. *Photochem. Photobiol.* **1987**, *46*, 707.

0022-3654/90/2094-5684$02.50/0